Stem Cell Research (2013) 11, 1250–1263

Available online at www.sciencedirect.com

ScienceDirect

www.elsevier.com/locate/scr

Adhesion, but not a specific cadherin code, is indispensable for ES cell and induced pluripotency

Ivan Bedzhov[a,b], Hani Alotaibi[a], M. Felicia Basilicata[a], Kerstin Ahlborn[a], Ewa Liszewska[c], Thomas Brabletz[d,e,f], Marc P. Stemmler[a,d,*]

[a] *Department of Molecular Embryology, Max-Planck Institute of Immunobiology and Epigenetics, Stuebeweg 51, D-79108 Freiburg, Germany*
[b] *Wellcome Trust/Cancer Research UK Gurdon Institute, Tennis Court Road, Cambridge CB2 1QN, UK*
[c] *Laboratory of Molecular and Cellular Neurobiology, The International Institute of Molecular and Cell Biology, 4 Ks. Trojdena Street, 02-109 Warsaw, Poland*
[d] *Department of Visceral Surgery, University Medical Center Freiburg, Hugstetter Str. 55, D-79106 Freiburg, Germany*
[e] *Comprehensive Cancer Center Freiburg, University Medical Center Freiburg, D-79106 Freiburg, Germany*
[f] *BIOSS Centre for Biological Signaling Studies, Albert-Ludwigs-University Freiburg, D-79104 Freiburg, Germany*

Received 5 February 2013; received in revised form 24 June 2013; accepted 17 August 2013
Available online 26 August 2013

Abstract Embryonic stem (ES) cell pluripotency and induced pluripotent stem (iPS) cell generation is dependent on a core transcriptional network and proper cell–cell adhesion mediated by E-cadherin (E-cad). Whereas E-cad is associated with pluripotency, *N-cadherin* (*N-cad*) expression is correlated with differentiation into mesodermal and neuroectodermal lineages. We investigated whether E-cad harbors unique molecular features in establishing or maintaining pluripotency. By using a gene replacement knock-in (ki) approach to express *N-cadherin* (*N-cad*) or E-cad/N-cad chimeric cadherins under the control of the *E-cad* locus, we show that all E-cad-depleted ki/ki ES cells are maintained in an undifferentiated state. Surprisingly, these cells retained key features of pluripotency, such as *Nanog* expression and full differentiation capacity in vitro and in vivo, whereas E-cad knockout (ko) ES cells irreversibly lost most of these features. Moreover, our results indicate that E-cad mediated adhesion is essential for iPS cell generation, since E-cad depleted fibroblasts were not reprogrammed. In contrast, N-cad efficiently supports somatic reprogramming similar to E-cad, and permits initiation of the crucial initial step of mesenchymal–epithelial transition. Thus, we show that cell adhesion and a robust pluripotent phenotype are ultimately connected. Since N-cad properly compensates for loss of E-cad, no specific 'cadherin code' is required.

Introduction

In mammalian cells, pluripotency is defined as the ability to self renew and to give rise to progenitors that differentiate into all cell types of the organism. This is best exemplified in the embryonic stem (ES) cells and blastocyst inner cell mass (ICM) cells that give rise to the embryo proper (Hanna et al.,

* Corresponding author at: Department of Molecular Embryology, Max-Planck Institute of Immunobiology and Epigenetics, Stuebeweg 51, D-79108 Freiburg, Germany. Fax: +49 761 5108 474.
E-mail address: stemmler@immunbio.mpg.de (M.P. Stemmler).

1873-5061/$ - see front matter © 2013 Elsevier B.V. All rights reserved.
http://dx.doi.org/10.1016/j.scr.2013.08.009

2010; Niwa, 2007). Pluripotency and the deprivation of embryonic stem cells are ultimately connected to a core transcriptional network, with Oct4, Sox2 and Nanog as central players (Hanna et al., 2010; Silva et al., 2009; Ying et al., 2008). The expression of these genes maintains an undifferentiated state that is characterized by key pluripotency gene activity, growth in dome-shaped colonies and the presence of bivalent chromatin marks on many promoters (Boyer et al., 2006; Mikkelsen et al., 2007). In vitro, the undifferentiated state is maintained by the activation of Lifr/gp130/p-STAT3 and a blockade of FGF4/p-ERK signaling to inhibit differentiation cues provided either by the presence of Lif and serum components/BMPs or by specific inhibitors (2i, 3i) in a chemically defined medium (Ying et al., 2008). A transcription factor cocktail comprised of Sox2, Klf4, Oct4 and c-Myc was successfully used to reprogram mouse somatic cells into cells that share many characteristics with ES cells and was thus defined to be necessary and sufficient to generate and maintain a pluripotent state, in ES or induced pluripotent cells (iPS cells) (Takahashi and Yamanaka, 2006; Wernig et al., 2007). Reprogramming is a gradual, multi-step process that is initiated by the downregulation of somatic genes as the epigenetic landscape of the genome is reset to a naive, ES cell-like state. Bivalent histone marks on lineage-associated genes are re-established and maintained by the action of Polycomb group proteins (Boyer et al., 2006; Maherali et al., 2007; Pereira et al., 2010). Early ES cell specific markers such as SSEA-1 and *Fbx15* are upregulated, followed by the reactivation of demethylated endogenous *Oct4*, *Sox2* and *Nanog* loci. The fibroblast-specific mesenchymal appearance is lost, and cells show signs of polarization during a mesenchymal to epithelial transition (MET) and a gain of ES cell-like morphology (Li et al., 2010). However, although individual steps of reprogramming have been uncovered, a complete understanding of how somatic cells become ES-like cells is still lacking.

During somatic reprogramming, a key step in completing MET is to establish cell adhesion and a more polarized phenotype, mainly mediated by the cell–cell adhesion glycoprotein E-cadherin (E-cad) (Stemmler, 2008). The loss of E-cad is associated with striking changes in intracellular adhesion that caused a dispersed single-cell appearance of cultured ES cells (Larue et al., 1996). Moreover, the expression of E-cad is also correlated with and required to maintain the ES cell ground state (Chou et al., 2008; Soncin et al., 2009), as well as to enhance fibroblast reprogramming (Chen et al., 2010). The presence of E-cad regulates the expression and the localization of key membrane proteins such as ZO-1, Eph receptors and the 5T4 oncofetal antigen (McNeill et al., 1990; Orsulic and Kemler, 2000; Spencer et al., 2007), indicating that it coordinates architectural changes. Hence, ES cell homeostasis ultimately depends on E-cad mediated cell–cell contacts and adhesion, which are required for communication and signaling. In contrast, mesenchymal cells, such as fibroblasts, express *N-cadherin* (*N-cad*). N-cad and E-cad have very similar activities in mediating homophilic cell adhesion and share the same intracellular binding partners, such as β-catenin, but are generally expressed in a mutually exclusive manner. In addition, these proteins coordinate distinct cellular phenotypes; E-cad usually induces a polarized epithelial shape, whereas N-cad is associated with a depolarized motile state (Stemmler, 2008; Wheelock et al., 2008). Accordingly, MET is one of the most essential steps during reprogramming to reach pluripotency. The elimination of potent epithelial to mesenchymal transition (EMT) inducers and E-cad repressors such as Snail, Slug and Zeb1 is required to efficiently shut down *N-cad* and to induce the expression of *E-cad*, a process that precedes the upregulation of endogenous *Oct4*, *Nanog* and *Sox2* (Li et al., 2010). Remarkably, it was recently shown that the forced expression of *E-cad* is sufficient to replace *Oct4* in the cocktail of Yamanaka factors and supports efficient reprogramming (Redmer et al., 2011). Thus, E-cad, which induces cell–cell contact formation, not only serves as a stemness marker but also contributes significantly to the acquisition and maintenance of pluripotency in iPS and ES cells. However, it remains unknown whether E-cad is a key molecule with unique properties or simply paves a path for reprogramming competence by supporting an adhesive phenotype.

We recently found that E-cad function cannot be replaced by N-cad during the formation of the trophectoderm, the first polarized epithelium formed during mammalian development. In the blastocyst, the E-cad extracellular domain provides a unique and indispensable survival signal by facilitating Igf1r signaling, in addition to its adhesive function (Bedzhov et al., 2012; Kan et al., 2007). Here, we investigated whether E-cad has a similarly unique function and governs a related process to promote ES cell identity and induced pluripotency. Our data confirmed and extended previous observations regarding the crucial function of E-cad during iPS cell deprivation and ES cell ground state maintenance (Chen et al., 2010; Redmer et al., 2011). However, although indispensable for these processes, our results suggest that E-cad function can be replaced by N-cad to rescue an undifferentiated pluripotent ES cell state. In addition, N-cad supports iPS cell generation, indicating that the establishment of cell contact formation and adhesion, rather than an E-cad specific induction of reprogramming, is crucial for this process.

Materials and methods

Mouse breeding and genotyping

Animal husbandry and all experiments were performed according to the German Animal Welfare guidelines and approved by the local authorities. Ncadki, NcGFP (Kan et al., 2007), E-cadHA (Stemmler and Bedzhov, 2010), EcNc, NcEc (Bedzhov et al., 2012), E-cad ko (Larue et al., 1994), E-cadflox and *Gt(ROSA)26Sor/J* (ROSA26) (Boussadia et al., 2002; Zambrowicz et al., 1997) mice were maintained in a C57BL/6 genetic background and crossed inter se. Genotyping was carried out as described previously (Bedzhov et al., 2012; Stemmler and Bedzhov, 2010).

Isolation and culture of ES cells

E2.5 embryos were isolated from heterozygous intercrosses. The zona pellucida was removed by a brief incubation in Tyrode's solution (Sigma-Aldrich Corporation). Single zona-free embryos were transferred to separate wells of 96-well plates containing ES cell medium (DMEM (Biochrom), 15% FCS (PAN), 10 U/ml Pen/Strep, 0.1 mM NEAA, 2 mM L-glutamine (Gibco), 0.15 mM β-mercaptoethanol (Sigma-Aldrich Corporation), 500 U/ml Lif (Millipore Corporation)) and mitotically inactivated embryonic fibroblasts. To increase the frequency of

ES cell derivation, the ES cell medium was supplemented with 50 μM MAPK inhibitor (PD98059, Calbiochem) and 5 μM GSK-3β inhibitor (SB216763, Sigma-Aldrich Corporation) during the initial blastocyst culturing steps and withdrawn after passaging. The embryos attached and formed outgrowths 3–4 days after plating. The outgrowths were trypsinized, and the cells were transferred to new wells with feeder cells. ES cell colonies became visible after 2–4 days.

iPS cell generation

Embryonic fibroblasts were obtained from E13.5 mice with E-cad ko/flox, E-cadHA ki/flox and N-cad ki/flox genotypes according to standard protocols. Fibroblasts were subjected to Adeno-Cre-mediated recombination with efficiencies of >90%, identified by genotyping (Akagi et al., 1997). Early passage E-cad ko/flox, E-cad ko/Δ, E-cadHA ki/Δ and N-cad ki/Δ fibroblasts (1×10^4 for lentiviral infection or 1.5×10^5 for plasmid transfection) were plated in 6-well plates. STEMCCA or pCAGMKOSiE expression plasmids, both containing *c-Myc*, *Klf4*, *Oct4* and *Sox2* coding sequences linked by the foot and mouth disease virus 2A peptide sequence, were used to reprogram embryonic fibroblasts according to previously reported protocols (Carey et al., 2009; Okita et al., 2010; Sommer et al., 2009).

AP staining

Cells were fixed in 4% PFA/PBS for 15 min and then washed twice with PBS. The cells were protected from light and incubated for 30 min in AP staining solution (25 mM Tris–maleic acid pH 9.0, 0.4 mg/ml α-naphthyl phosphate, 1 mg/ml Fast Red TR salt, 8 mM $MgCl_2$, 0.01% Na-deoxycholate, 0.02% NP-40). The reaction was stopped by H_2O, followed by two washes in PBS.

Immunofluorescence labeling and confocal microscopy

Cells were washed with PBS and fixed with ice-cold methanol for 20 min at room temperature. After washing twice with PBS, cells were incubated with primary antibody in PBS (1:200) for 2 h to overnight at room temperature. Subsequently, Alexa488 or Alexa594-conjugated secondary antibodies were applied for 1 h. Cells were stained with DAPI to visualize nuclei (1:1000, Invitrogen Corporation) and mounted on a microscope slide. Confocal microscopy was performed using Zeiss Spinning Disc system. Images were processed using IMARIS software (Bitplane). The antibodies used were: anti-E-cadherin, anti-N-cadherin (BD Biosciences), HA.11 (Covance), anti-Sox2 (Calbiochem), anti-Oct4, anti-GATA-4 (Santa Cruz Biotechnology, Inc.), anti-Nestin (Chemicon International, Inc.), anti-β tubulin III, anti-GFAP (Sigma-Aldrich Corporation), anti-Vimentin (EXBIO Praha), TROMA-1 (Kemler et al., 1981), anti-Nanog (Messerschmidt and Kemler, 2010), and anti-SSEA-1, previously reported as ECMA-7 (Kemler et al., 1981).

ES cell differentiation in vitro

Undifferentiated ES cells (5×10^4) were suspended in 5 ml differentiation medium (DMEM, 20% FCS, 10 U/ml Pen/Strep, 0.15 mM β-mercaptoethanol). Then, 30 μl drops (approximately 300 cells per drop) was placed on the undersurface of the lid of a 100 mm tissue culture dish. The lid was inverted and placed on the top of a dish containing 10 ml of PBS. Simple embryoid bodies (EBs) were formed after 2 days of incubation at 37 °C and 8% CO_2. On the third day, the drops were collected and transferred into a 100 mm bacterial petri dish with 10 ml differentiation medium. After 3 days of incubation, the simple EBs were transferred to gelatin-coated glass cover slips in each well of a 24 well tissue culture plate. Cardiac myocyte contraction was evident 4 to 7 days after plating. If kept in suspension, the simple EBs transform into cystic EBs after 8–11 days.

Teratoma formation

BALB/c nude mice were injected subcutaneously with 1×10^7 ES cells. Solid tumors were isolated 3 weeks after injection. The teratomas were fixed in 4% PFA/PBS overnight and embedded into paraffin.

Generation of chimeric embryos and β-galactosidase histochemistry

ES cell injection into N-cad ki/+ host blastocysts and embryo analysis was performed as described (Kan et al., 2007).

Paraffin embedding and immunohistochemistry

Specimens were fixed at 4 °C overnight in 4% PFA/PBS. The samples were dehydrated in an ethanol series (30%, 50%, 70% and 100% in PBS) for 2 h each, followed by two 10 min incubations in 100% xylene, and then transferred to paraffin overnight. Samples casted into paraffin blocks were sectioned at 7 μm using a RM2155 microtome (Leica). Hematoxylin/eosin staining and immunohistochemistry were carried out as described previously; epitope retrieval was performed by boiling for 20 min in Tris-EDTA pH 9.0 buffer (Libusova et al., 2010; Stemmler and Bedzhov, 2010).

mRNA expression analysis

RNA was prepared from sub-confluent cultures grown in 6-well plates using the Nucleospin RNA II kit (Macherey-Nagel GmbH & Co.) as recommended by the manufacturer. RNA was quantified using the NanoDrop 2000 (Thermo Scientific). One microgram of total RNA was used for cDNA synthesis using the Maxima First Strand cDNA Synthesis kit (Fermentas). Primers and probes used for qPCR are presented in Supplementary Table S2. Quantitative RT-PCR was performed using the ABsolute QPCR ROX mix (Thermo Scientific) and amplification was performed in the 7300 Real time PCR system (Applied Biosystems) using the following cycling parameters: 95 °C 15 min, 40 cycles of 95 °C 15 s, 60 °C 45 s. Relative expression to the WT control (+/+) was calculated using the ΔΔCt method and normalized to *Gapdh* expression. Data represent 3 biological replicates. Statistical analysis was done by applying 1-way ANOVA and Tukey's Multiple Comparison Test.

Microarray analysis

Microarray analysis was performed with two RNA samples per genotype. RNA concentration and quality was assessed using a NanoDrop 2000 instrument. Hybridization to the GeneChip Mouse Genome 430 v2.0 arrays (Affymetrix, Inc.) was performed by Atlas Biolabs GmbH (Berlin, Germany), and these data are accessible through GEO Series accession number GSE42008 (http://www.ncbi.nlm.nih.gov/geo/query/acc.cgi?acc=GSE42008). For the E-cad ko and WT (D3) genotypes, raw data from Soncin et al. (2011) was used. Data analysis was performed using R/Bioconductor Limma software. The quality of the data set was controlled through the simpleaffy package and normalized by quantile normalization with the GCRMA algorithm. Log2-transformed normalized expression values of the selected gene sets were used to generate a heatmap image. Hierarchical clustering was performed with Pearson's correlation.

Results

Switching *E-cad* expression to ectopic cadherins did not affect ES cell derivation

To investigate the specific function of E-cad in ES cell maintenance and pluripotency, we used a previously described E-cad gene replacement approach. The E-cad (*Cdh1*) locus was targeted by different constructs. Knock-in (ki) alleles carrying sequence insertions resulting in the control of the ki gene expression by E-cad regulatory elements and the simultaneous inactivation of E-cad expression. Sequences coding for untagged (N-cad ki) or tagged N-cad (N-cadGFP) (Kan et al., 2007), hemagglutinin (HA)-tagged chimeric cadherins (EcNc and NcEc) (Bedzhov et al., 2012) and a control allele containing wild-type (WT) E-cad were used (E-cadHA) (Stemmler and Bedzhov, 2010) (Figs. 1A and B, Supplementary Figs. S1A and B). Corresponding homozygous ES cell lines were isolated from blastocyst outgrowths, genotyped and analyzed for protein expression from the *Cdh1* locus (Supplementary Fig. S4). To determine whether the generated cells were true ES cells, we analyzed the morphology of the colonies as a first criterion. All ki/ki ES cell lines displayed proper compact dome-shaped appearance, similar to that of WT controls (Fig. 1C). In the N-cad ki/ki, N-cadGFP ki/ki, EcNc ki/ki and NcEc ki/ki lines, the degree of cell separation was slightly increased. In contrast, E-cad ko cells grew as single cells without a typical dome-shaped colony appearance (Fig. 1C). This finding is consistent with previous observations (Bedzhov et al., 2012; Kan et al., 2007; Larue et al., 1996; Stemmler and Bedzhov, 2010). To verify the appropriate expression of the knocked-in cadherins, ES cells were immunofluorescently labeled. N-cad and N-cadGFP were properly localized to the cell membrane in the absence of endogenous E-cad (not shown and Fig. 1D), and similar observations were made for the chimeric cadherins and the control E-cadHA (Fig. 1E). In contrast, E-cad ko ES cells were devoid of *E-cad* expression (Larue et al., 1996) (Fig. 1F). This indicated that ES cell morphology is strongly dependent on cadherin-mediated cell adhesion and that it can be rescued by N-cad, EcNc and NcEc. N-cad and chimeric proteins in the ki/ki ES cells properly maintained adhesion and a compact colony architecture, the fundamental morphological characteristics of WT ES cells.

Expression of the pluripotency circuit is maintained by N-cad or the chimeric cadherins in the absence of endogenous E-cad

In agreement with our morphological observations, all homozygous ki ES cells showed alkaline phosphatase (AP) activity, another criterion often used to identify pluripotent stem cells (Fig. 2A). AP staining was absent from E-cad ko ES cells, indicating that they are not pluripotent and have lost their ES cell characteristics. In a more thorough analysis, we performed a global transcriptome analysis to determine whether E-cad replacement caused minor changes in cell identity. We compared the gene expression profiles of N-cadGFP ki/+ and N-cadGFP ki/ki to WT (W4) ES cells. Previously published expression profiles of WT (D3) and E-cad ko ES cells were also included in the microarray analysis (Soncin et al., 2011) (Fig. 2B). Key pluripotency and differentiation genes were used as the basis of a clustering analysis of the different ES cells. The expression profiles of the W4, heterozygous and homozygous NcadGFP ES cells were grouped in close proximity to that of D3, the second WT line. This group was clearly separated from the replicates of the E-cad ko cell expression profile (Fig. 2B). Consistent with this cluster analysis, no striking difference in the expression of pluripotency-associated genes was observed among both WT lines, N-cadGFP ki/+ and N-cadGFP ki/ki ES cells. Likewise, genes that were upregulated during differentiation into derivatives of the three germ layers or extraembryonic tissues remained unchanged overall. In contrast, the separate clustering of E-cad ko ES cells was also reflected in the altered expression of genes associated with the pluripotency network. With the exception of *Oct4*, a general downregulation of pluripotency genes, especially of the transcription factors *Nanog*, *Klf4* and *Tbx3*, was detected, confirming a previous analysis (Soncin et al., 2011). Epiblast stem cell-specific genes, such as *Fgf5*, as well as certain ectoderm and mesoderm-specific genes, such as *Nef3*, *Galr2*, *T-Bra* and *Eomes*, were upregulated. Quantitative real-time PCR analysis confirmed that the core pluripotency factors were expressed at comparable levels between the homo-, heterozygous N-cad ki and WT ES cells. In stark contrast, in the E-cad ko ES cells, *Sox2* and *Nanog* were downregulated and *Klf4* and *Tbx3* were virtually absent (Fig. 2C), and *Fgf5* was induced 15-fold. Similar results were obtained in analyses of Oct4, Nanog and Sox2 protein expression and in the detection of the pluripotency-associated glycosphingolipid SSEA-1. Consistently, immunofluorescence labeling and confocal imaging revealed comparable intensities in all ES cell lines, with the exception of E-cad ko, which showed a significant reduction in the expression of all analyzed markers. Notably, SSEA-1 was undetectable (Fig. 2D; Supplemental Fig. S2A and data not shown). Ezrin and ZO-1, which are molecular markers of cell polarity and tight junctions, respectively, were present and properly localized in WT and all ki ES cells but nearly undetectable in E-cad ko cells (Supplemental Fig. S3).

These results show that proper cell–cell contacts and cell interactions are essential for the stable expression of the transcription factors that determine the pluripotent state of

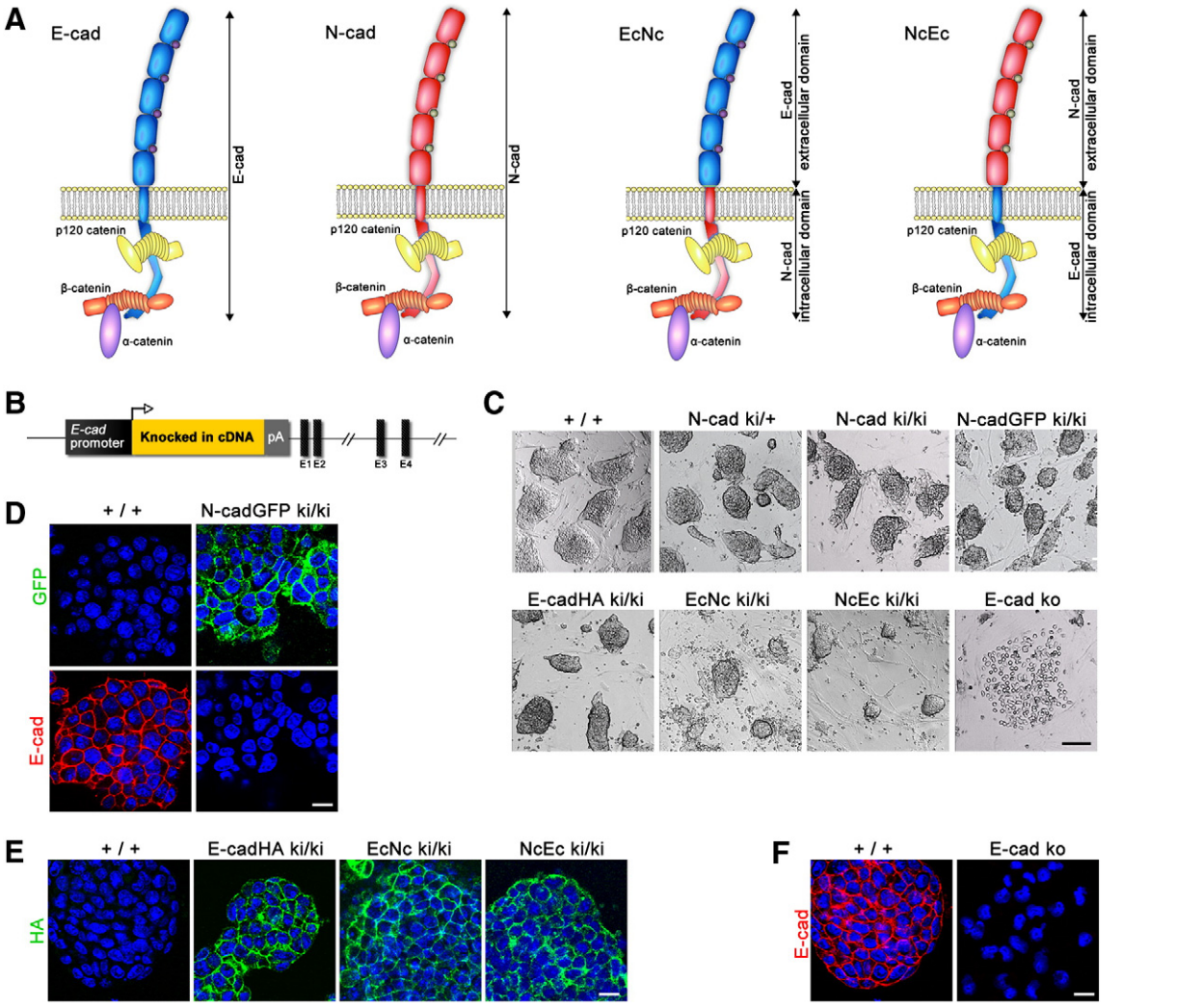

Figure 1 Expression of the ki cadherins in homozygous ES cells. (A) Schematic representation of E-cad, N-cad, EcNc and NcEc proteins in complex with catenins. (B) General scheme of a ki allele in the E-cad locus, pA (SV40 polyadenylation signal), E1-4 (E-cad exons). (C) Brightfield images of homozygous ES cells expressing N-cad, N-cadGFP, E-cadHA or the chimeric cadherins growing in compacted colonies in contrast to E-cad ko ES cells. Scale bar — 200 μm. (D) Optical confocal section of N-cadGFP ki/ki and WT (+/+) ES cells immunolabeled for GFP (green) and E-cad (red). (E) Anti-HA immunofluorescence staining (green) of WT, E-cadHA, EcNc and NcEc homozygous ES cells. (F) Optical confocal sections of WT and E-cad ko ES cells stained for E-cad (red). Nuclei are counterstained with DAPI. Scale bar — 15 μm.

the ES cells. In this context, the function of E-cad is exchangeable; the normal pluripotency network is maintained if the cells are held together either by N-cad or by the artificial chimeric cadherins. In ES cells, E- to N-cad switching did not trigger differentiation and maintained adhesion, in contrast to the downstream cascades initiated by cadherin switching during EMT in the process of gastrulation or tumorigenesis, which result in depolarization and migration.

Figure 2 Factors determining the pluripotent state are properly expressed and maintained in the homozygous ki ES cells. (A) AP-positive WT, N-cad, N-cadGFP, E-cadHA, EcNc and NcEc ki/ki colonies with typical ES cell morphology in comparison to E-cad ko AP-negative ES cells. Scale bar — 200 μm. (B) Heat map of microarray gene expression analysis comparing relative transcript levels of factors associated with pluripotency and factors, specific for the embryonic (ecto, endo and mesoderm) and the extraembryonic (trophectoderm) lineages in WT (D3), WT (W4), N-cad heterozygous (ki/+), N-cad homozygous (ki/ki) and E-cad ko ES cells. Red represents high and green low expression levels. Dendrogram of hierarchal clustering of 12 individual microarrays are given (see Supplemental Table S1 for RMA values). Two arrays per genotype represent biological replicates in WT (W4), N-cad ki/+ and N-cad ki/ki. Three arrays per genotype represent biological replicates in WT (D3) and E-cad ko. (C) Quantitative RT-PCR validation of the microarray data of ES-cell specific genes (Supplemental Table S2), relative to *Gapdh*, error bars represent SEM from three independent experiments; *Oct4*, $p = 0.1149$; *Sox2*, $p = 0.0003$; *Nanog*, $p = 0.0045$; *Klf4*, $p < 0.0001$; *Tbx3*, $p = 0.0045$; *Fgf5*, $p = 0.0176$. (D) Optical confocal sections of ES cells stained for Oct4 (red), Nanog (green) and Sox2 (red). Scale bar — 15 μm.

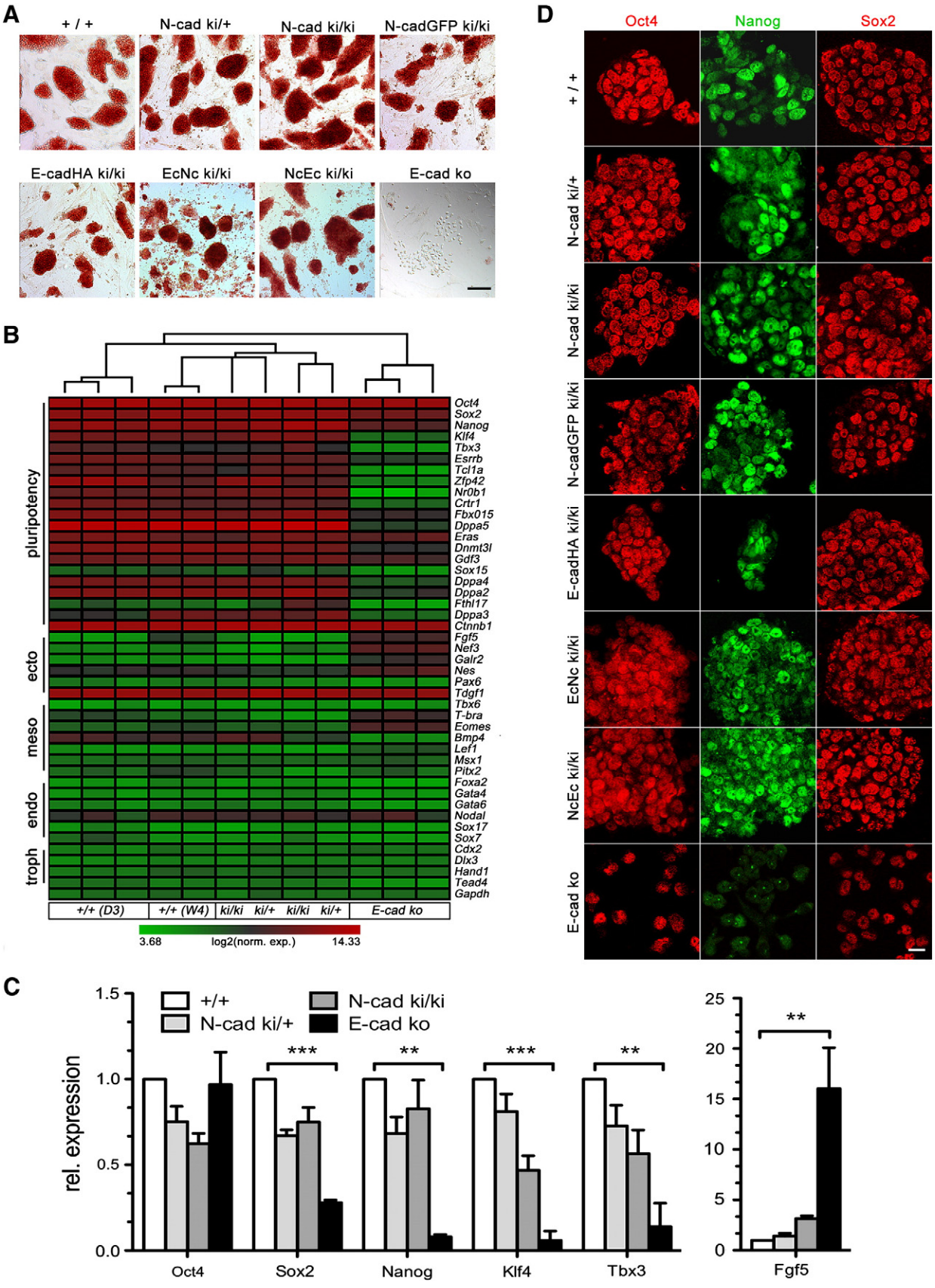
A
+ / +
N-cad ki/+
N-cad ki/ki
N-cadGFP ki/ki
E-cadHA ki/ki
EcNc ki/ki
NcEc ki/ki
E-cad ko
B
pluripotency
ecto
meso
endo
troph
Oct4
Sox2
Nanog
Klf4
Tbx3
Esrrb
Tcl1a
Zfp42
Nr0b1
Crtr1
Fbx015
Dppa5
Eras
Dnmt3l
Gdf3
Sox15
Dppa4
Dppa2
Fthl17
Dppa3
Ctnnb1
Fgf5
Nef3
Galr2
Nes
Pax6
Tdgf1
Tbx6
T-bra
Eomes
Bmp4
Lef1
Msx1
Pitx2
Foxa2
Gata4
Gata6
Nodal
Sox17
Sox7
Cdx2
Dlx3
Hand1
Tead4
Gapdh
+/+ (D3)
+/+ (W4)
ki/ki
ki/+
ki/ki
ki/+
E-cad ko
3.68
log2(norm. exp.)
14.33
D
Oct4
Nanog
Sox2
+ / +
N-cad ki/+
N-cad ki/ki
N-cadGFP ki/ki
E-cadHA ki/ki
EcNc ki/ki
NcEc ki/ki
E-cad ko
C
+/+
N-cad ki/+
N-cad ki/ki
E-cad ko
rel. expression
1.5
1.0
0.5
0.0
***
**
***
**
Oct4
Sox2
Nanog
Klf4
Tbx3
25
20
15
10
5
0
**
Fgf5

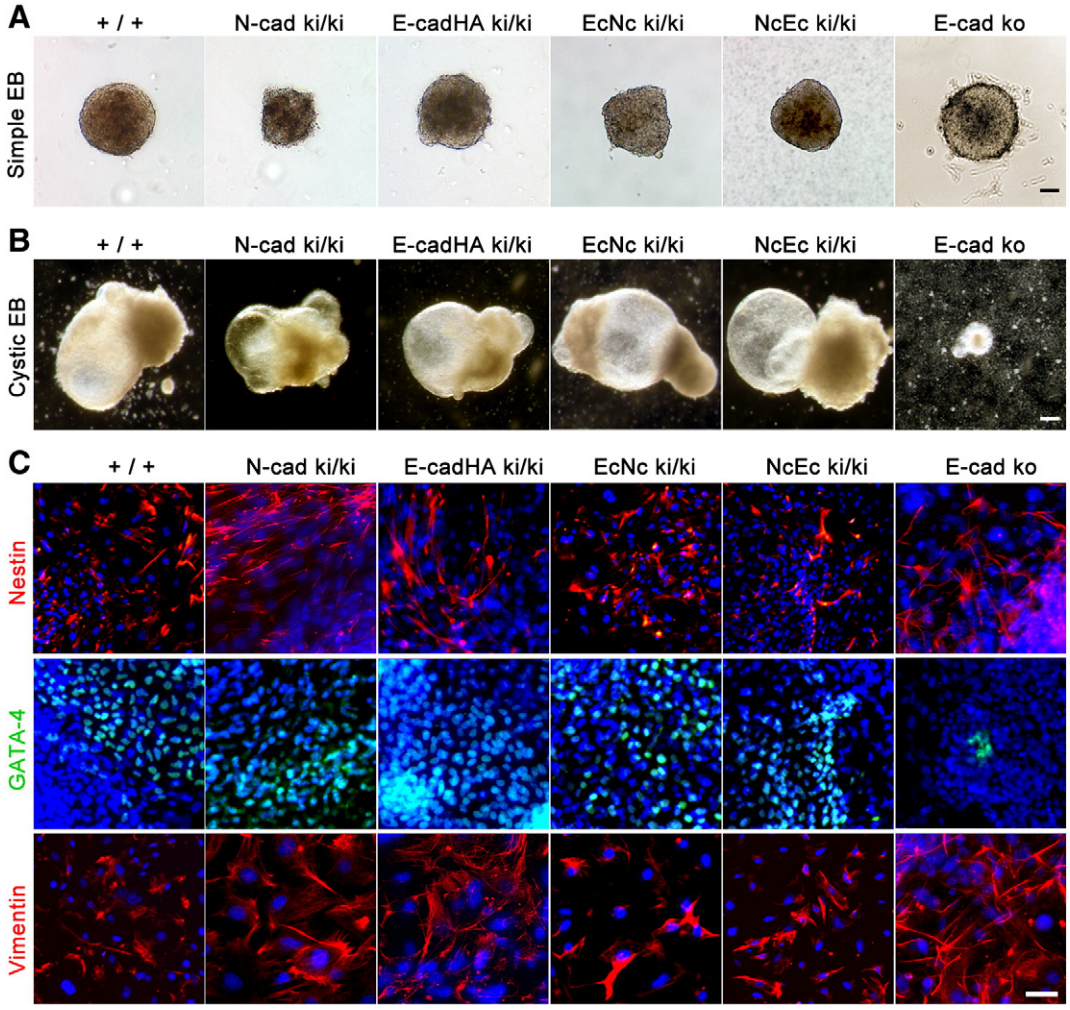

Figure 3 In vitro differentiation of ES cells in EB assay. (A) Simple EBs formed by ES-cell aggregation in a hanging drop culture in the absence of Lif and feeders. Scale bar — 50 μm. (B) Cystic EBs with visceral yolk sack structures generated from WT, N-cad, E-cadHA, EcNc and NcEc ki/ki simple EB. E-cad ko simple EBs remained small and failed to form cysts. Scale bar — 200 μm. (C) Derivatives of the three germ layers revealed by antibody staining for Nestin (ectoderm), GATA-4 (endoderm) and Vimentin (mesoderm). Nuclei are counterstained with DAPI. Scale bar — 40 μm.

N-cad ki/ki, EcNc ki/ki and NcEc ki/ki ES cells demonstrate normal differentiation competence, in contrast to E-cad ko

To analyze whether the different homozygous ki ES cells were competent to differentiate into derivatives of the three germ layers, we induced a synchronous differentiation. When cultured in hanging drops in differentiating medium for 3–6 days, all mutant cell lines formed spheroid aggregates of a similar size, classified as simple embryoid bodies (EBs). Surprisingly, even in the absence of E-cad in E-cad ko cells, the rounded bottom of the hanging drop allowed the formation of compact aggregates, most likely mediated by other adhesive molecules that are upregulated during differentiation (Fig. 3A). After 8–11 days in suspension, WT simple EBs transform into cystic EBs containing visceral yolk sac membranes (Doetschman et al., 1985). Similar structures were found in all genotypes, except for the EBs derived from E-cad ko ES cells. Primary E-cad ko EBs remained small, failed to form and expand visceral yolk sac cysts and showed an increase in apoptotic/necrotic cells (Fig. 3B). Upon the transfer of simple EBs to an adhesive gelatin-coated culture dish, differentiated cells migrate out of the aggregate and spread. We characterized the lineage composition of these cells using a set of well-established marker genes to determine whether early embryonic differentiation is recapitulated. Cells expressing Nestin, a marker for ectoderm-derived neural stem cells, were found in all analyzed cell lines (Fig. 3C). GATA4, a transcription factor present in definitive endoderm derivatives and upregulated in the anterior lateral plate mesoderm during heart formation, was detected in patches of cells spread from WT and all homozygous mutant ki variants. In contrast, only small clusters of 10–30 GATA4-positive cells were found in E-cad ko-derived EBs (Fig. 3C). Cells of mesodermal origin identified by anti-Vimentin immunoreactivity were detected in all genotypes (Fig. 3C). However, contracting foci of beating cardiomyocytes, an indication of (terminal) mesoderm differentiation, were observed only in WT and ki outgrowths and were absent from E-cad ko cultures (Supplemental Movies S1–S5). These results show that all ki cell lines exhibit a differentiation capacity indistinguishable from that of WT

ES cells and that this differentiation potential is affected by the absence of adhesion mediated by classical cadherins. The narrower spectrum of lineage differentiation of E-cad ko ES cells might be due to changes in the pluripotency network that already primed the differentiation towards certain fates. This hypothesis is further supported by the observed upregulation of the lineage-specific genes *Fgf5*, *T-Bra*, *Eomes* and *Lef1* under standard ES cell culture conditions.

Inappropriate cadherin expression does not affect the proper differentiation of ES cells in vivo

Teratomas and chimeric embryos were generated to further examine the pluripotency of the ki/ki ES cell lines with exchanged adhesion signatures in vivo. All ki ES cells formed solid teratomas of similar sizes to those formed by the WT control. Smaller tumors were obtained from E-cad ko ES cells (Supplemental Fig. S2B). Histological analysis of sections of WT, N-cadGFP ki/ki, E-cadHA ki/ki, EcNc ki/ki and NcEc ki/ki teratomas revealed tissues with characteristic structures of all three germ layers (Fig. 4A). Intensively hematoxylin-stained neuroepithelium forming immature neural tubes of ectoderm, gut-like structures with columnar epithelium and cysts of endodermal and cartilage and muscle of mesodermal origin were identified (Fig. 4A). In agreement with the previous analysis, E-cad ko teratomas appeared to be poorly differentiated (Larue et al., 1996). Only N-cad-positive radial structures of columnar cells resembling neural rosettes and neural tubes were visible (Fig. 4A). The capacity of N-cadGFP ki/ki and E-cad ko ES cells to differentiate towards the neural lineage was confirmed by GFAP and β-tubulin III staining, showing that this route of differentiation is not affected in any of the analyzed ES cells (Fig. 4B). Similarly, Vimentin-positive mesenchymal cells were found in all homozygous ki and E-cad ko ES cell-derived teratomas, whereas no muscle or cartilage were found in E-cad ko samples (Figs. 4A and B). N-cadGFP, E-cadHA, EcNc and NcEc expression was restricted to epithelial structures that were positive for cytokeratin 8 (detected by TROMA-1), recapitulating the endogenous expression pattern of E-cad. No ectopic expression was found in the surrounding stroma, indicating the proper regulation of the ki cadherins, as reported previously (Bedzhov et al., 2012; Kan et al., 2007) (Figs. 4C–E).

In a more stringent in vivo assay, the homozygous ki ES cells were tested for their ability to contribute to chimeric embryos. Heterozygous blastocysts co-expressing E-cad and N-cad were used to permit the integration of N-cad ki/ki ES cells into the host epiblast. ROSA26 host blastocysts with constitutive *lacZ*-expression allowed the detection of ES cell-derived cells in chimeric embryos at E8.5 (Fig. 5A). Whereas E-cad ko ES cells were incapable of contributing to the embryo proper (data not shown), ES cell-derived progeny of N-cad ki/ki without β-galactosidase activity populated all three germ layers (Fig. 5B, arrows), although with a lower efficiency than observed for heterozygous ES cells (Figs. 5C and D). No obvious preference in the differentiation of N-cad ki/ki ES cells towards certain germ layers or embryonic structures was observed. These results confirmed that N-cad ki/ki ES cells are a true pluripotent source of ecto-, endo- and mesoderm and are properly specified in vivo, whereas E-cad ko ES cells are not.

E-cad-mediated adhesion is indispensable for fibroblast reprogramming but can be replaced by N-cad

Our data strongly indicate that ES cell pluripotency is fundamentally based on the maintenance of E-cad mediated adhesion. The heterotypic expression of another classical cadherin, N-cad, can compensate for the loss of E-cad to maintain ES cell identity. Next, we tested whether this is also true during induced pluripotency. We introduced the Yamanaka factors into isolated E-cad ko/flox, N-cad ki/Δ and E-cad ko/Δ embryonic fibroblasts generated by Adeno-Cre-mediated E-cad depletion. Lentiviral infection or transfection with a single expression plasmid containing *c-Myc*, *Klf4*, *Oct4* and *Sox2* yielded similar results (Carey et al., 2009; Okita et al., 2010; Sommer et al., 2009). We hypothesized that the endogenous *N-cad* in fibroblasts would be downregulated during reprogramming-induced MET and that this change, combined with an activation of the *E-cad* locus, would lead to endogenous *E-cad* or *N-cad* expression from the ki allele (Fig. 6A). The reprogramming capacity was monitored based on appearance of dome-shaped ES cell-like colonies and staining for AP-positive cell clusters. Although the number of generated iPS colonies was five times lower in N-cad ki/Δ, AP-positive iPS colonies emerged with 0.5% efficiency, reaching a ratio similar to that observed for E-cad ko/flox controls (Fig. 6B). Consistent with the data presented above, the reprogramming of E-cad ko/Δ fibroblasts was severely compromised in this bulk analysis. A decrease from 90% to 50% AP+-colonies in N-cad ki/Δ or E-cad ko/flox was detected (Fig. 6B).

Six colonies were randomly picked from each genotype prior to AP staining and analyzed for E-cad and Nanog expression as well as for AP activity. Because 5–10% of cells remained unrecombined upon Adeno-Cre-mediated E-cad depletion (not shown), the iPS colonies of N-cad ki/Δ and E-cad ko/Δ were first tested for E-cad expression to eliminate false positives. For both lines, three out of six iPS clones showed an absence of E-cad; the remaining escapers from Cre-mediated E-cad depletion were excluded from further analysis (Fig. 6B). Clones were verified by PCR genotyping and protein analysis, showing proper recombination of the E-cadflox allele and protein expression of the knock-in allele reduced to about 50% in comparison to ES cells due to monoallelic expression (Supplementary Fig. S4). All six E-cad ko/flox iPS cells displayed pluripotency based on anti-Nanog, SSEA-1 and AP staining (Figs. 6C–E). Consistent with the previous results, N-cad ki/Δ fibroblasts were successfully reprogrammed, as evident by *Nanog* expression and AP activity. However, growth in separated cells after plating was detected and compact colony formation required extra time. This difference between N-cad ki/Δ iPS and N-cad ki/ki ES cells is likely due to a gene dosage effect, with lower expression from only one copy in N-cad ki/Δ iPS cells (Supplementary Fig. S4). In contrast to N-cad ki/Δ iPS cells, E-cad ko/Δ transfected fibroblasts formed colonies that were negative for SSEA-1, Nanog and AP (Figs. 6C–E), confirming that they began proliferating to form colonies but were incapable of establishing a pluripotent iPS cell state. This was further confirmed by analyzing the

pluripotency capacity of generated iPS clones in vivo and in vitro. Teratomas successfully formed from E-cad ko/flox, E-cadHA ki/Δ and N-cad ki/Δ clones, but not upon injection of E-cad ko/Δ cells (Supplementary Fig. S5). These teratomas showed a similar differentiation potential of N-cad ki/Δ as of E-cad ko/flox and E-cadHA ki/Δ iPS cells. We also examined the differentiation capacity of iPS cells in vitro by EB formation. As anticipated, E-cad ko/flox, E-cadHA ki/Δ and N-cad ki/Δ iPS cells generated EBs from which migrating cells, positive for differentiation markers, were detected (Supplemental Fig. S6).

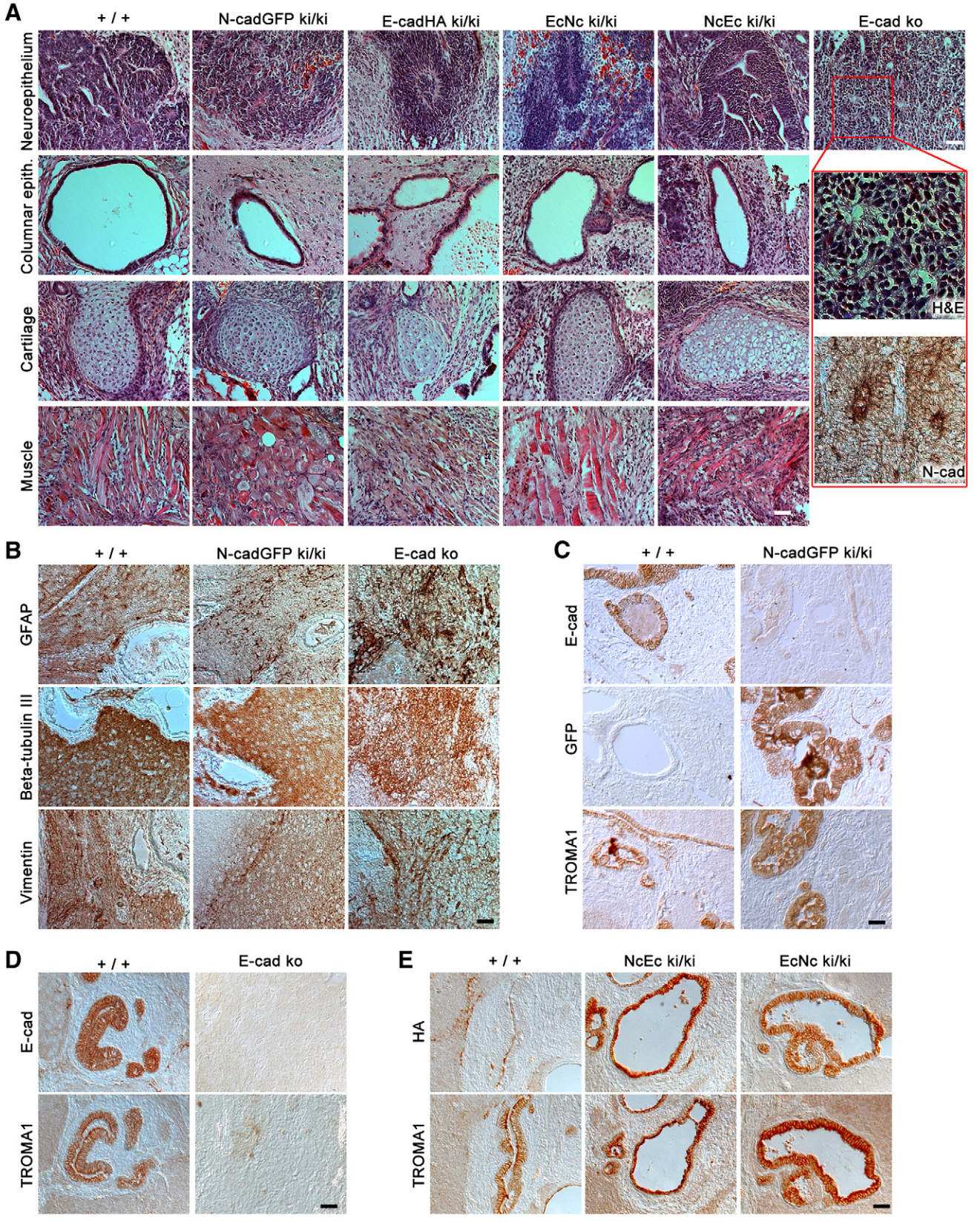

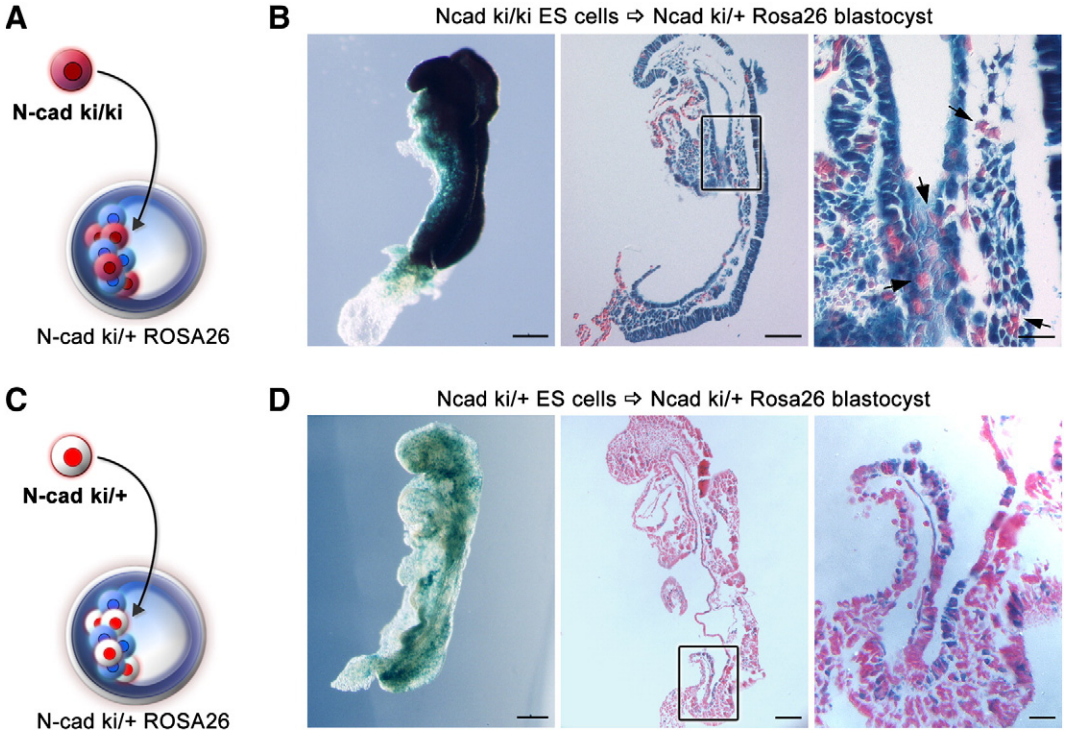

Figure 5 N-cad ki/ki and ki/+ ES-cell contribution to chimeric embryos. (A) X-gal staining of a representative E8.5 chimeric embryo obtained from N-cad ki/ki ES-cell injection. The embryo was sectioned and counterstained with eosin. The progeny of the N-cad ki/ki ES cells contributing to the three germ layers is β-galactosidase negative (arrows). (B) X-gal staining of E8.5 chimeric embryo generated from N-cad ki/+ ES-cell injection. β-galactosidase negative cells, derived from the injected ES cells, were found in all three germ layers. Scale bars from left to right panels — 250, 100, 25 μm, respectively.

Although EBs of E-cad ko/Δ cells were also formed and cells migrated away from the EB after plating, they showed only limited immunoreactivity to specific differentiation markers. This shows that a cadherin-mediated cell adhesion is indispensable for complete somatic cell reprogramming (Fig. 6A). However, the function of E-cad in this process is exchangeable. The induction of MET, which is crucial for efficient reprogramming, can also be achieved in the presence of ectopic N-cad. Presumably, adhesion and the modulation of the cytoskeleton are required, rather than a unique function of E-cad.

Discussion

Unraveling the ground state of ES cell pluripotency and the ability to reprogram differentiated cells paved the way for regenerative medicine with the potential to use patient-derived cells with ES cell properties. The pathways and regulators that maintain ES cell pluripotency are still ill defined, and a better understanding of the mechanisms underlying pluripotency and differentiation is necessary (Ying et al., 2008). E-cad is important for the maintenance of proper ES cell pluripotency and is able to enhance the generation of iPS cells, in which it can replace Oct4 in the Yamanaka cocktail of pluripotency factors (Chen et al., 2010; Redmer et al., 2011; Soncin et al., 2009). Reprogramming requires an initial MET. This essential step seems to be highly dynamic with phases of both EMT and MET and cadherins play a very important role during this process (Liu et al., 2013). In fibroblast, directly after viral transduction of the pluripotency genes, temporal activation of *Snai2* expression was observed. Consequently, further activation of *N-cad* and repression of *E-cad* in an EMT-like process was detectable, important for efficient reprogramming, before MET is stabilized during days 3–5. Here, we investigated the specific requirements of E-cad in ES cell pluripotency and during reprogramming. Our results show that pluripotency and differentiation capacity are maintained in ES cells that exclusively express N-cad or chimeric E-cad/N-cad proteins with swapped extracellular domains. The proper induction of pluripotency, which requires the exogenous expression of *Oct4*, *Sox2* and *Nanog*, was detected in genetically modified fibroblasts that switch from endogenous *N-cad* to *N-cad* expression from a ki allele during initial MET. In contrast,

Figure 4 Differentiation capacity in vivo in teratoma formation assay. (A) Hematoxylin/eosin (H&E) staining on paraffin sections revealing structures of neuroepithelium, columnar epithelium, cartilage and muscle in WT, N-cadGFP ki/ki, E-cadHA ki/ki, EcNc ki/ki and NcEc ki/ki teratomas. Neural rosettes in E-cad ko teratomas stained for H&E and N-cad. (B) Neural tissues positive for beta tubulin III and GFAP and mesenchymal tissues stained for Vimentin in WT, N-cadGFP ki/ki and E-cad ko teratomas. (C) N-cadGFP expression restricted to TROMA-1 positive epithelial structures. (D) WT and E-cad ko teratomas stained for E-cad and TROMA-1. (E) Consecutive sections showing HA and TROMA-1 positive epithelial structures in EcNc and NcEc ki/ki teratomas. Scale bars — 100 μm.

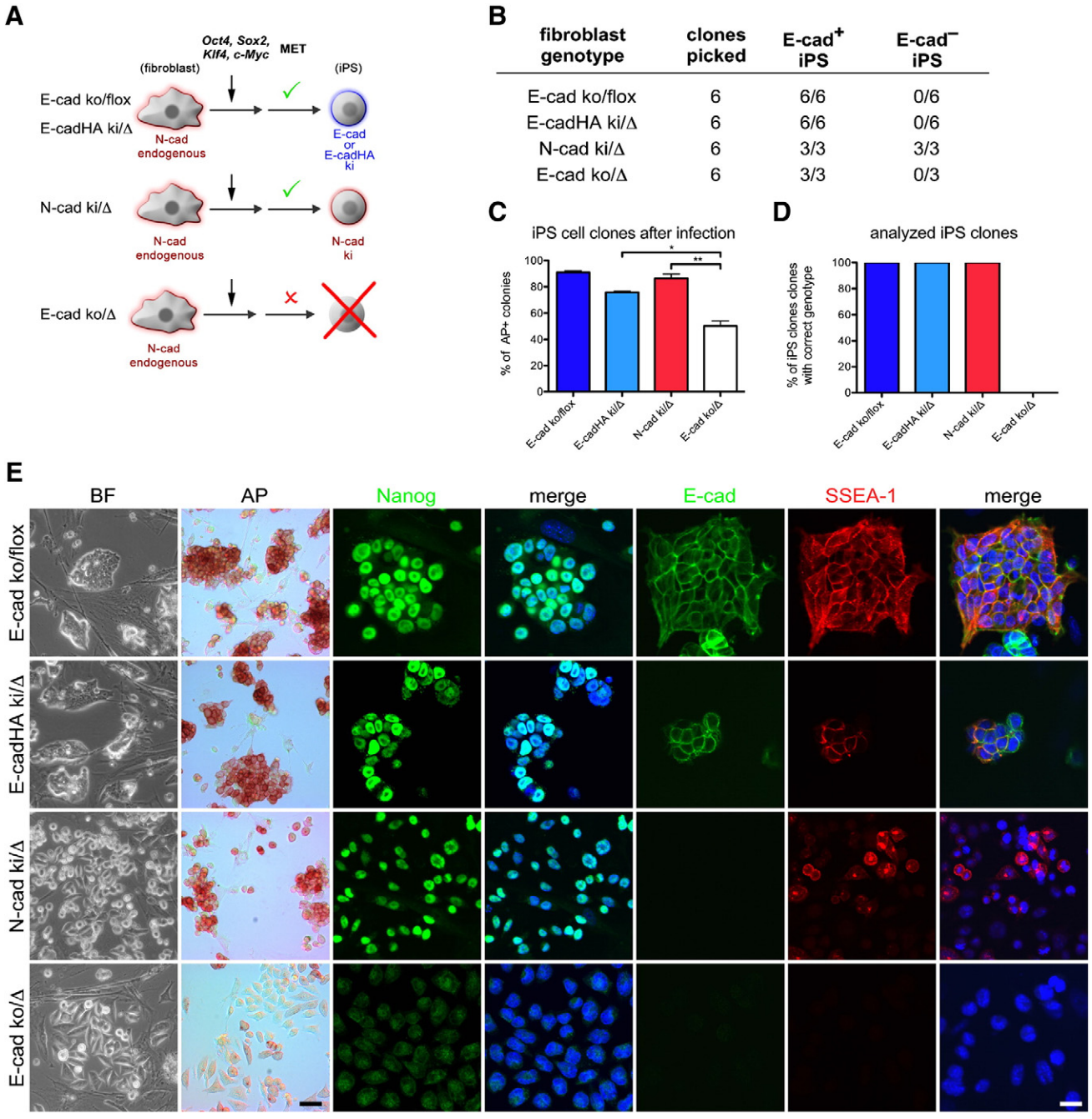

Figure 6 N-cad can substitute for E-cad function during reprogramming. (A) Scheme of reprogramming in different isolated embryonic fibroblasts. Red or blue shadow highlights N-cad and E-cad expression, respectively, driven by endogenous or ki loci. (B) Table summarizing results of picked and analyzed clones after reprogramming. (C, D) Ratio of iPS colonies in the bulk screen (C) and after detailed analysis of individual clones for E-cad, Nanog and SSEA-1 immunoreactivity. Error bars represent SEM; p = 0.0014 (D). Note, that after normalization and excluding unrecombined E-cadflox clones, no E-cad-depleted iPS cells were found in E-cad ko/Δ transfectants. (E) Bright field image, AP staining and optical confocal sections of immunofluorescence analysis of SSEA-1, E-cad and Nanog expression and AP activity in analyzed iPS-cell clones of indicated genotypes. Nanog- and AP-positive clones were present in N-cad ki/Δ but absent from E-cad ko/Δ transfectants. Nuclei are counterstained with DAPI. Scale bars from left to right panels — 50, 15 μm, respectively.

E-cad ko ES cells lost key features of pluripotency and differentiation capacity. Consistent with these findings, no iPS cells were obtained from E-cad ko/Δ fibroblasts. Thus, pluripotency is ultimately connected to cell–cell adhesion for ES cell maintenance and induced pluripotency during the initiation of MET. Moreover, our results show that N-cad-mediated adhesion can replace the function of E-cad in ES and iPS cells, suggesting that the maintenance or

establishment of cell adhesion and a specific cytoskeletal architecture that permits cells to cluster and form compact colonies is a fundamental process. This phenomenon blocks differentiation in ES cells and allows efficient reprogramming.

The presence of E-cad stabilizes the expression and controls the localization of ZO-1, Eph receptors and the 5T4 oncofetal antigen, supporting the role of E-cad in guiding and coordinating protein localization to remodel the cellular architecture (Orsulic and Kemler, 2000; Spencer et al., 2007). Klf4 was shown to bind to the E-cad promoter and directly activate E-cad transcription during the initial events of fibroblast reprogramming (Chen et al., 2010; Li et al., 2010). In line with this observation, epithelial cells that already express E-cad and Klf4 endogenously, such as keratinocytes, show increased reprogramming capabilities, with greater than 100-fold higher efficiency than mesenchymal cell-originated fibroblasts (Aasen et al., 2008). This indicates that, in fibroblasts, the initial expression of endogenous *N-cad* is not sufficient to support reprogramming, whereas the *N-cad* expressed from our ki allele is capable of efficiently promoting MET during this process.

In contrast, it is very surprising that N-cad can confer a compact ES cell phenotype and is capable of participating in the MET process in our gene replacement approach. With the exception of its expression in the pseudostratified neuroepithelium, N-cad is usually associated with a mesenchymal unpolarized cell phenotype. During vertebrate gastrulation, mesodermal cells acquire a migratory phenotype only upon proper E-cad downregulation and de novo N-cad expression (Carver et al., 2001). MET processes, such as those observed during uretic bud morphogenesis in kidney development, require an opposite switching of cadherin expression (Vestweber et al., 1985). Similar observations have been made during epithelial-derived tumor progression. In these tumors, invasion and metastasis are correlated with cadherin expression switching and changes in cell shape from an E-cad^{+}N-cad^{-} sessile well-polarized epithelial phenotype to an E-cad^{-}N-cad^{+} depolarized motile mesenchymal phenotype (Lim and Thiery, 2012; Stemmler, 2008; Thiery et al., 2009). In contrast to these analyses, the switch in cadherin expression during iPS cell induction in N-cad ki/Δ fibroblasts is only apparent on the genomic level. When endogenous *N-cad* is silenced, the activation of the *E-cad* locus leads to *N-cad* expression from the ki allele, which does not consequently affect the protein type. This supports the hypothesis that, in this context, the entire MET program rather than simple cadherin expression may support cadherin function in cell adhesion and the acquisition of an apical–basal polarized cell shape, instead of the maintenance of a mesenchymal fibroblast-like phenotype, as occurs in the neuroectoderm. Once MET is initiated, the cells can utilize either E-cad or N-cad to stabilize the more epithelial phenotype.

We succeeded in generating iPS cells from N-cad ki/Δ fibroblasts; however, we noticed a reduction in efficiency in comparison to WT control cells. In addition, although we cannot completely rule out the possibility of a bias toward the selection of nicely shaped E-cad^{+} iPS cells during the colony picking procedure, we found that half of the isolated iPS cell clones emerged from the small cell population that evaded Cre-mediated E-cad depletion. This observation suggests that the depleted cells are more difficult to reprogram than are control cells. This might be due to different expression levels of the ki alleles compared to endogenous E-cad expression, as identified previously (Bedzhov et al., 2012; Stemmler and Bedzhov, 2010) or to differences in the adhesive strength of the cadherin molecules. Under specific conditions, N-cad was found to provide less adhesive strength than E-cad using atomic force measurements to separate two adherent cells (Chu et al., 2004, 2006). Moreover, whereas the lower *E-cad* gene dosage in E-cad ko/+ compared with E-cad +/+ ES cells does not result in reduced adhesion and different morphology, striking differences in colony formation between N-cad ki/ki ES and N-cad ki/Δ iPS cells were detected. A combination of the lower expression of the ki allele and the putative reduced adhesive force of N-cad may explain why biallelic and monoallelic expressions in this case reduce cell adhesion. However, no loss of pluripotency marker expression was observed in the analyzed N-cad ki/Δ iPS cells, indicating that sufficient N-cad protein and adhesion was present.

Our results indicate that the pivotal role of E-cad in establishing and maintaining pluripotency can also be provided by N-cad. Interestingly, this is in contrast to the function of E-cad during preimplantation development, during which E-cad is required to facilitate Igf1r signaling. The genetic ablation of E-cad first affects the trophectoderm (TE) lineage and induces apoptosis, whereas the ICM, the pluripotent lineage within the embryo that is closely related to ES cells, is affected later (Stephenson et al., 2010). Applying the ki approach to preimplantation development showed that N-cad cannot substitute for E-cad function during TE formation. Although N-cad maintained cell–cell adhesion, apoptosis was induced, as in the TE lineage, whereas the ICM was unaffected and ES cell derivation was possible (Bedzhov et al., 2012; Kan et al., 2007). In addition, the differential interaction of E-cad and N-cad with individual receptor tyrosine kinases, such as EGFR and members of the FGFR family, has been found to have several consequences on both adhesion and on signaling in other cellular systems (Fedor-Chaiken et al., 2003; Hoschuetzky et al., 1994; Pece and Gutkind, 2000; Qian et al., 2004; Suyama et al., 2002). To highlight these unique and specific functions of E-cad and N-cad that are independent of their role in cell adhesion we use the term "cadherin code". Surprisingly, the cadherin code is not required for ES cell and induced pluripotency, and cadherin function is interchangeable. Because the initial step of reprogramming requires MET combined with cytoskeletal rearrangements and cell clustering, it is tempting to speculate that the adhesive function and the anchorage to the cytoskeleton via β-catenin are crucial but can be accomplished by both cadherin molecules. This process, which presumably acts via β-catenin and Lifr-mediated STAT3 phosphorylation, occurs at both types of adherens junctions, as shown recently by Hawkins et al. (2012). Alternatively, Lifr may interact directly with either E-cad or N-cad, and only the complete absence of both cadherins can block STAT3 phosphorylation (del Valle et al., 2013). Consequently, the transcriptome of E-cad ko ES cells is dramatically altered, and pluripotency is lost (Soncin et al., 2011). Interestingly, under conditions using chemically defined media complemented with BMP4 and LIF or in 3i medium, endogenous *N-cad* expression is upregulated in E-cad ko ES cells, resulting in a partial re-expression of *Nanog* and increases in p-STAT3 levels (Hawkins et al., 2012). However, the inability of E-cad ko cells to switch to uniform and robust

Nanog expression and their dependence on special culturing conditions indicate that the underlying mechanisms acting in ES cells and during the initial MET process in reprogrammed cells are complex and are not determined by the presence or absence of cadherins alone.

Cadherin-mediated cell adhesion is indispensable for pluripotency in ES cells and iPS cell generation. However, whether appropriate Lifr/gp130/p-STAT3 pathway activation is ultimately connected to cadherins or whether these molecules only glue cells together, in combination with intracellular protein rearrangements, remains unknown. In this context, it would be very interesting to see whether any cell–cell adhesion molecule, such as EpCAM, is able to rescue pluripotency in a similar manner as N-cad.

In conclusion, our data show that adhesion is indispensable for pluripotency and that E-cad is the major mediator of this adhesion. However, this function is not unique and can be carried out by N-cad, indicating that no specific cadherin (cadherin code) is required. The results presented here provide further insight into the cellular mechanisms that are involved in regulating the ES cell ground state and activated during reprogramming, revealing in more detail the importance of cell adhesion.

Supplementary data to this article can be found online at http://dx.doi.org/10.1016/j.scr.2013.08.009.

Acknowledgments

We thank Kati Hansen and Robert Kuhnert for excellent technical assistance and Rolf Kemler for helpful discussions and sharing reagents. We are grateful to Benoît Kanzler and Caroline Johner from the transgenic and animal facilities at MPI IE. This work was supported by the Max Planck Society and the Deutsche Forschungsgemeinschaft SFB850 TP A4.

References

Aasen, T., Raya, A., Barrero, M.J., Garreta, E., Consiglio, A., Gonzalez, F., Vassena, R., Bilic, J., Pekarik, V., Tiscornia, G., et al., 2008. Efficient and rapid generation of induced pluripotent stem cells from human keratinocytes. Nat. Biotechnol. 26, 1276–1284.

Akagi, K., Sandig, V., Vooijs, M., Van der Valk, M., Giovannini, M., Strauss, M., Berns, A., 1997. Cre-mediated somatic site-specific recombination in mice. Nucleic Acids Res. 25, 1766–1773.

Bedzhov, I., Liszewska, E., Kanzler, B., Stemmler, M.P., 2012. IGF1R signaling is indispensable for preimplantation development and is activated via a novel function of E-cadherin. PLoS Genet. 8, e1002609.

Boussadia, O., Kutsch, S., Hierholzer, A., Delmas, V., Kemler, R., 2002. E-cadherin is a survival factor for the lactating mouse mammary gland. Mech. Dev. 115 (1–2), 53–62.

Boyer, L.A., Plath, K., Zeitlinger, J., Brambrink, T., Medeiros, L.A., Lee, T.I., Levine, S.S., Wernig, M., Tajonar, A., Ray, M.K., et al., 2006. Polycomb complexes repress developmental regulators in murine embryonic stem cells. Nature 441, 349–353.

Carey, B.W., Markoulaki, S., Hanna, J., Saha, K., Gao, Q., Mitalipova, M., Jaenisch, R., 2009. Reprogramming of murine and human somatic cells using a single polycistronic vector. Proc. Natl. Acad. Sci. U.S.A. 106, 157–162.

Carver, E.A., Jiang, R., Lan, Y., Oram, K.F., Gridley, T., 2001. The mouse snail gene encodes a key regulator of the epithelial–mesenchymal transition. Mol. Cell. Biol. 21, 8184–8188.

Chen, T., Yuan, D., Wei, B., Jiang, J., Kang, J., Ling, K., Gu, Y., Li, J., Xiao, L., Pei, G., 2010. E-cadherin-mediated cell–cell contact is critical for induced pluripotent stem cell generation. Stem Cells 28, 1315–1325.

Chou, Y.F., Chen, H.H., Eijpe, M., Yabuuchi, A., Chenoweth, J.G., Tesar, P., Lu, J., McKay, R.D., Geijsen, N., 2008. The growth factor environment defines distinct pluripotent ground states in novel blastocyst-derived stem cells. Cell 135, 449–461.

Chu, Y.S., Thomas, W.A., Eder, O., Pincet, F., Perez, E., Thiery, J.P., Dufour, S., 2004. Force measurements in E-cadherin-mediated cell doublets reveal rapid adhesion strengthened by actin cytoskeleton remodeling through Rac and Cdc42. J. Cell Biol. 167, 1183–1194.

Chu, Y.S., Eder, O., Thomas, W.A., Simcha, I., Pincet, F., Ben-Ze'ev, A., Perez, E., Thiery, J.P., Dufour, S., 2006. Prototypical type I E-cadherin and type II cadherin-7 mediate very distinct adhesiveness through their extracellular domains. J. Biol. Chem. 281, 2901–2910.

del Valle, I., Rudloff, S., Carles, A., Li, Y., Liszewska, E., Vogt, R., 2013. E-cadherin is required for the proper activation of the Lifr/Gp130 signaling pathway in mouse embryonic stem cells. Development 140 (8), 1684–1692.

Doetschman, T.C., Eistetter, H., Katz, M., Schmidt, W., Kemler, R., 1985. The in vitro development of blastocyst-derived embryonic stem cell lines: formation of visceral yolk sac, blood islands and myocardium. J. Embryol. Exp. Morphol. 87, 27–45.

Fedor-Chaiken, M., Hein, P.W., Stewart, J.C., Brackenbury, R., Kinch, M.S., 2003. E-cadherin binding modulates EGF receptor activation. Cell Commun. Adhes. 10, 105–118.

Hanna, J.H., Saha, K., Jaenisch, R., 2010. Pluripotency and cellular reprogramming: facts, hypotheses, unresolved issues. Cell 143, 508–525.

Hawkins, K., Mohamet, L., Ritson, S., Merry, C.L., Ward, C.M., 2012. E-cadherin and, in its absence, N-cadherin promotes Nanog expression in mouse embryonic stem cells via STAT3 phosphorylation. Stem Cells 30, 1842–1851.

Hoschuetzky, H., Aberle, H., Kemler, R., 1994. Beta-catenin mediates the interaction of the cadherin–catenin complex with epidermal growth factor receptor. J. Cell Biol. 127, 1375–1380.

Kan, N.G., Stemmler, M.P., Junghans, D., Kanzler, B., de Vries, W.N., Dominis, M., Kemler, R., 2007. Gene replacement reveals a specific role for E-cadherin in the formation of a functional trophectoderm. Development 134, 31–41.

Kemler, R., Brulet, P., Schnebelen, M.T., Gaillard, J., Jacob, F., 1981. Reactivity of monoclonal antibodies against intermediate filament proteins during embryonic development. J. Embryol. Exp. Morphol. 64, 45–60.

Larue, L., Ohsugi, M., Hirchenhain, J., Kemler, R., 1994. E-cadherin null mutant embryos fail to form a trophectoderm epithelium. Proc. Natl. Acad. Sci. U.S.A. 91, 8263–8267.

Larue, L., Antos, C., Butz, S., Huber, O., Delmas, V., Dominis, M., Kemler, R., 1996. A role for cadherins in tissue formation. Development 122, 3185–3194.

Li, R.H., Liang, J.L., Ni, S., Zhou, T., Qing, X.B., Li, H.P., He, W.Z., Chen, J.K., Li, F., Zhuang, Q.A., et al., 2010. A mesenchymal-to-epithelial transition initiates and is required for the nuclear reprogramming of mouse fibroblasts. Cell Stem Cell 7, 51–63.

Libusova, L., Stemmler, M.P., Hierholzer, A., Schwarz, H., Kemler, R., 2010. N-cadherin can structurally substitute for E-cadherin during intestinal development but leads to polyp formation. Development 137, 2297–2305.

Lim, J., Thiery, J.P., 2012. Epithelial–mesenchymal transitions: insights from development. Development 139, 3471–3486.

Liu, X., Sun, H., Qi, J., Wang, L., He, S., Liu, J., 2013. Sequential introduction of reprogramming factors reveals a time-sensitive

requirement for individual factors and a sequential EMT–MET mechanism for optimal reprogramming. Nat. Cell Biol. http://dx.doi.org/10.1038/ncb2765.

Maherali, N., Sridharan, R., Xie, W., Utikal, J., Eminli, S., Arnold, K., Stadtfeld, M., Yachechko, R., Tchieu, J., Jaenisch, R., et al., 2007. Directly reprogrammed fibroblasts show global epigenetic remodeling and widespread tissue contribution. Cell Stem Cell 1, 55–70.

McNeill, H., Ozawa, M., Kemler, R., Nelson, W.J., 1990. Novel function of the cell adhesion molecule uvomorulin as an inducer of cell surface polarity. Cell 62, 309–316.

Messerschmidt, D.M., Kemler, R., 2010. Nanog is required for primitive endoderm formation through a non-cell autonomous mechanism. Dev. Biol. 344, 129–137.

Mikkelsen, T.S., Ku, M., Jaffe, D.B., Issac, B., Lieberman, E., Giannoukos, G., Alvarez, P., Brockman, W., Kim, T.K., Koche, R.P., et al., 2007. Genome-wide maps of chromatin state in pluripotent and lineage-committed cells. Nature 448, 553–560.

Niwa, H., 2007. How is pluripotency determined and maintained? Development 134, 635–646.

Okita, K., Hong, H., Takahashi, K., Yamanaka, S., 2010. Generation of mouse-induced pluripotent stem cells with plasmid vectors. Nat. Protoc. 5, 418–428.

Orsulic, S., Kemler, R., 2000. Expression of Eph receptors and ephrins is differentially regulated by E-cadherin. J. Cell Sci. 113 (Pt 10), 1793–1802.

Pece, S., Gutkind, J.S., 2000. Signaling from E-cadherins to the MAPK pathway by the recruitment and activation of epidermal growth factor receptors upon cell–cell contact formation. J. Biol. Chem. 275, 41227–41233.

Pereira, C.F., Piccolo, F.M., Tsubouchi, T., Sauer, S., Ryan, N.K., Bruno, L., Landeira, D., Santos, J., Banito, A., Gil, J., et al., 2010. ESCs require PRC2 to direct the successful reprogramming of differentiated cells toward pluripotency. Cell Stem Cell 6, 547–556.

Qian, X., Karpova, T., Sheppard, A.M., McNally, J., Lowy, D.R., 2004. E-cadherin-mediated adhesion inhibits ligand-dependent activation of diverse receptor tyrosine kinases. EMBO J. 23, 1739–1748.

Redmer, T., Diecke, S., Grigoryan, T., Quiroga-Negreira, A., Birchmeier, W., Besser, D., 2011. E-cadherin is crucial for embryonic stem cell pluripotency and can replace OCT4 during somatic cell reprogramming. EMBO Rep. 12, 720–726.

Silva, J., Nichols, J., Theunissen, T.W., Guo, G., van Oosten, A.L., Barrandon, O., Wray, J., Yamanaka, S., Chambers, I., Smith, A., 2009. Nanog is the gateway to the pluripotent ground state. Cell 138, 722–737.

Sommer, C.A., Stadtfeld, M., Murphy, G.J., Hochedlinger, K., Kotton, D.N., Mostoslavsky, G., 2009. Induced pluripotent stem cell generation using a single lentiviral stem cell cassette. Stem Cells 27, 543–549.

Soncin, F., Mohamet, L., Eckardt, D., Ritson, S., Eastham, A.M., Bobola, N., Russell, A., Davies, S., Kemler, R., Merry, C.L., et al., 2009. Abrogation of E-cadherin-mediated cell–cell contact in mouse embryonic stem cells results in reversible LIF-independent self-renewal. Stem Cells 27, 2069–2080.

Soncin, F., Mohamet, L., Ritson, S., Hawkins, K., Bobola, N., Zeef, L., Merry, C.L.R., Ward, C.M., 2011. E-cadherin acts as a regulator of transcripts associated with a wide range of cellular processes in mouse embryonic stem cells. PLoS One 6.

Spencer, H.L., Eastham, A.M., Merry, C.L., Southgate, T.D., Perez-Campo, F., Soncin, F., Ritson, S., Kemler, R., Stern, P.L., Ward, C.M., 2007. E-cadherin inhibits cell surface localization of the pro-migratory 5T4 oncofetal antigen in mouse embryonic stem cells. Mol. Biol. Cell 18, 2838–2851.

Stemmler, M.P., 2008. Cadherins in development and cancer. Mol. Biosyst. 4, 835–850.

Stemmler, M.P., Bedzhov, I., 2010. A Cdh1HA knock-in allele rescues the Cdh1 −/− phenotype but shows essential Cdh1 function during placentation. Dev. Dyn. 239, 2330–2344.

Stephenson, R.O., Yamanaka, Y., Rossant, J., 2010. Disorganized epithelial polarity and excess trophectoderm cell fate in preimplantation embryos lacking E-cadherin. Development 137, 3383–3391.

Suyama, K., Shapiro, I., Guttman, M., Hazan, R.B., 2002. A signaling pathway leading to metastasis is controlled by N-cadherin and the FGF receptor. Cancer Cell 2, 301–314.

Takahashi, K., Yamanaka, S., 2006. Induction of pluripotent stem cells from mouse embryonic and adult fibroblast cultures by defined factors. Cell 126, 663–676.

Thiery, J.P., Acloque, H., Huang, R.Y., Nieto, M.A., 2009. Epithelial–mesenchymal transitions in development and disease. Cell 139, 871–890.

Vestweber, D., Kemler, R., Ekblom, P., 1985. Cell-adhesion molecule uvomorulin during kidney development. Dev. Biol. 112, 213–221.

Wernig, M., Meissner, A., Foreman, R., Brambrink, T., Ku, M., Hochedlinger, K., Bernstein, B.E., Jaenisch, R., 2007. In vitro reprogramming of fibroblasts into a pluripotent ES-cell-like state. Nature 448, 318–324.

Wheelock, M.J., Shintani, Y., Maeda, M., Fukumoto, Y., Johnson, K.R., 2008. Cadherin switching. J. Cell Sci. 121, 727–735.

Ying, Q.L., Wray, J., Nichols, J., Batlle-Morera, L., Doble, B., Woodgett, J., Cohen, P., Smith, A., 2008. The ground state of embryonic stem cell self-renewal. Nature 453, 519–523.

Zambrowicz, B.P., Imamoto, A., Fiering, S., Herzenberg, L.A., Kerr, W.G., Soriano, P., 1997. Disruption of overlapping transcripts in the ROSA beta geo 26 gene trap strain leads to widespread expression of beta-galactosidase in mouse embryos and hematopoietic cells. Proc. Natl. Acad. Sci. U.S.A. 94, 3789–3794.